Collapse of Thermal Activation in Moderately Damped Josephson Junctions

V. M. Krasnov,[1] T. Bauch,[2] S. Intiso,[2] E. Hürfeld,[2] T. Akazaki,[3] H. Takayanagi,[3] and P. Delsing[2]

[1]*Department of Physics, Stockholm University, Albanova University Center, SE-10691 Stockholm, Sweden*

[2]*Department of Microtechnology and Nanoscience, Chalmers University of Technology, SE-41296 Göteborg, Sweden*

[3]*NTT Basic Research Laboratories, 3-1 Morinosato-Wakamiya, Atsugi-Shi, Kanagawa 243-01, Japan*

(Received 28 February 2005; published 6 October 2005)

We study switching current statistics in moderately damped Nb-InAs-Nb and intrinsic $Bi_2Sr_2CaCu_2O_{8+\delta}$ Josephson junctions. A paradoxical collapse of thermal activation with increasing temperature is reported and explained by the interplay of two conflicting consequences of thermal fluctuations, which can both assist in premature escape and help in retrapping back into the stationary state. We analyze the influence of dissipation on the thermal escape by tuning damping with a gate voltage, magnetic field, temperature, and an *in situ* capacitor.

DOI: 10.1103/PhysRevLett.95.157002 PACS numbers: 74.72.Hs, 74.40.+k, 74.45.+c, 74.50.+r

Dissipation plays a crucial role in decay of metastable states, which determines dynamics of various physical and chemical processes [1]. Switching between superconducting (S) and resistive (R) states in Josephson junctions (JJ's) is one of the best studied examples of such a decay. The influence of dissipation on the switching statistics of JJ's has been intensively studied both theoretically [1–4] and experimentally [5–10]. Electrodynamics of JJ's is equivalent to motion of a particle in a tilted washboard potential formed by superposition of the periodic Josephson potential and the work done by the current source (the tilt); see Fig. 3(c). The particle can escape from the potential well as a result of macroscopic quantum tunneling (MQT) or thermal activation (TA). At low damping the escaped particle will roll down the potential (switch to the R state). However, if dissipation exceeds the work done by the current source, it will be retrapped in subsequent wells (return to the S state).

The role of dissipation in decoherence of quantum systems [11] has recently become an important issue for quantum computing. JJ's are used in several different ways in qubit implementations. For example, current biased JJ's are employed in phase qubits [12], where the dissipation affects relaxation and decoherence in the qubits. Furthermore, switching of JJ's is also used for readout of both flux [13] and charge-phase [14] qubits.

So far switching statistics was studied for superconductor-insulator-superconductor (SIS) junctions, while superconductor–normal metal–superconductor (SNS) junctions, which are characterized by stronger dissipation effects, remain unstudied. Analysis of dissipation effects in SIS junctions is complicated by an ill-defined damping factor, which cannot be represented by a simple constant [4]. Conflicting reports exist on what determines the effective damping in SIS junctions: the normal resistance [5], the high frequency impedance of circuitry [6], or the quasiparticle resistance [7]. This ambiguity does not exist for SNS junctions with a typical resistance, R, much smaller than the open space impedance 377 Ω.

Here we study switching statistics in moderately damped Nb-InAs-Nb superconductor–two-dimensional electron gas–superconductor (S-2DEG-S) and $Bi_2Sr_2CaCu_2O_{8+\delta}$ (Bi-2212) high-T_c intrinsic Josephson junctions (IJJ's). Being able to tune the damping parameter by a gate voltage, a magnetic field, a temperature, and an *in situ* shunting capacitor, we analyze the influence of dissipation on switching statistics. For both systems we observe a sudden collapse of TA with increasing T and explain this paradoxical phenomenon by the interplay of two conflicting consequences of thermal fluctuations, which on one hand assist in premature switching and on

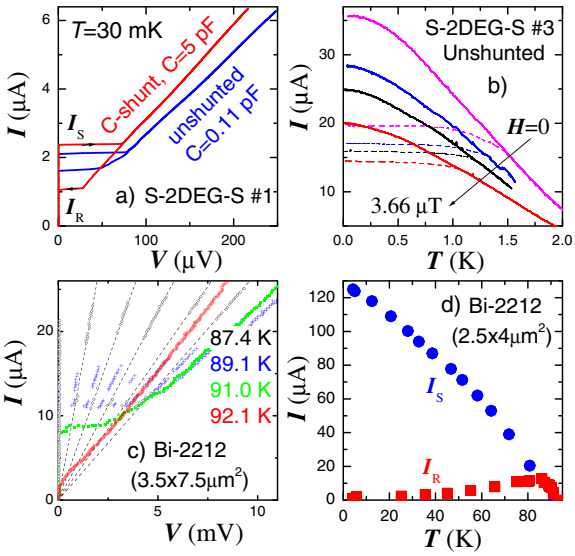

FIG. 1 (color online). (a) IVC's of S-2DEG-S No. 1 at $T =$ 30 mK before and after *in situ* C shunting. (b) Measured switching I_S (solid lines) and retrapping I_R (dashed lines) currents of S-2DEG-S No. 3 at four magnetic fields. (c) IVC's of a Bi-2212 mesa with nine IJJ's at four different $T < T_c \simeq 93$ K. Multibranch structure is due to one-by-one switching of IJJ's. (d) Measured I_S and I_R vs T for another mesa.

the other hand help in retrapping back to the S state. We present numeric and analytic calculations that are in good agreement with our experimental data [15].

Figure 1 shows current-voltage characteristics (IVC's) for 1(a) a S-2DEG-S junction No. 1 and 1(c) a Bi-2212 mesa with 9 stacked IJJ's. Details of sample fabrication can be found elsewhere [16–19]. Figures 1(b) and 1(d) show T dependencies of switching, I_S, and retrapping, I_R, currents for different JJ's. From Fig. 1 it is seen that the IVC's exhibit hysteresis and are well described by the resistively and capacitively shunted junction (RCSJ) model with constant damping [20]; see inset of Fig. 3(c). According to the RCSJ model the hysteresis is related to damping and appears when the quality factor of the junction (the inverse of the damping parameter) $Q_0 = \omega_{p0}RC$ is $\gtrsim 1$. Here $\omega_{p0} = (2eI_{c0}/\hbar C)^{1/2}$ is the Josephson plasma frequency, C is the junction capacitance, and I_{c0} is the fluctuation-free critical current. For Bi-2212, experimental I_S/I_R agrees well with the calculated Q_0 using capacitance of IJJ's $C \simeq 68.5\ \mathrm{fF}/\mu\mathrm{m}^2$ [19]. For the unshunted S-2DEG-S No. 1 from Fig. 1(a) the $I_S/I_R \simeq 1.3$ would correspond to $Q_0 = 1.4$ and $C \simeq 0.11$ pF, consistent with the estimated value of stray capacitance.

However, hysteresis in SNS JJ's is a controversial issue and can also be caused by self-heating [21], nonequilibrium effects [22], or frequency dependent damping [4]. To clarify the origin of hysteresis, we fabricated an *in situ* shunt capacitor, consisting of Al_2O_3/Al double layer deposited right on top of S-2DEG-S JJ's. The IVC's of the JJ No. 1 before and after C shunting are shown in Fig. 1(a). It is seen that I_S/I_R increased considerably, while R was little affected by C shunting. This indicates that the hysteresis is predominantly due to finite $Q_0 > 1$, rather than self-heating; see also Ref. [23].

S-2DEG-S provide a unique opportunity to tune the Josephson coupling energy E_{J0} and damping by applying gate voltage V_g [16,17]. For this a thin gate electrode was made on top of the InAs. Figure 2(a) shows switching current histograms for S-2DEG-S No. 2 at different V_g. The inset shows the width at the half-height, ΔI, versus the most probable switching current $I_{S\max}$. It is seen that initially histograms are getting wider with increasing negative V_g, consistent with the increase of TA with decreasing E_{J0}/T. However, at $V_g < -0.35$ V a sudden change occurs and ΔI starts to rapidly collapse.

Figure 2(b) shows ΔI vs T for the S-2DEG-S No. 3 at $H = 0, 2.32, 3.05$, and $3.66\ \mu$T, the same as in Fig. 1(b). In all cases we can distinguish three T regions: (i) At low T, ΔI is independent of T. The decrease of ΔI with H leaves no doubts that we observe the MQT regime [3–6] despite not very well defined quantum levels in our moderately damped SNS JJ's. (ii) At intermediate T, ΔI increases in agreement with TA calculations, shown by dashed lines in Fig. 2(c), for which the escape rate is given by the Arrhenius law

$$\Gamma_{\mathrm{TA}} = a_t \frac{\omega_p}{2\pi} \exp\left[-\frac{\Delta U}{k_B T}\right]. \quad (1)$$

Here ΔU is the potential barrier and $\omega_p = \omega_{p0}[1 - (I/I_{c0})^2]^{1/4}$. Damping enters only into the prefactor of Eq. (1), which for our moderately damped JJ's is $a_t = (1 + 1/4Q^2)^{1/2} - 1/2Q$ [3], where $Q = \omega_p RC$. (iii) At higher T, the histograms start to rapidly collapse leading to a downturn of ΔI. This paradoxical phenomenon is the cental observation of our work.

Figure 3(d) shows a similar collapse for IJJ's. In this case $T^* \sim 75$ K is close to $T_c \simeq 93$ K. Since ΔI may decrease together with I_{c0} at $T \to T_c$, here we show the effective escape temperature T_{esc}, obtained by fitting experimental histograms using Eq. (1). By definition, $T_{\mathrm{esc}} \equiv T$ for conventional TA, which is indeed the case for $T < T^*$, see the dashed line in Fig. 3(d). Therefore, the drastic drop in T_{esc} at $T > T^*$, cannot be explained within a simple TA scenario. Similar conclusions can be drawn in all other cases from comparison with TA predictions shown by dashed lines in Figs. 2(c), 4(b), and 4(c).

Figures 3(a) and 3(b) show switching histograms of a *single* IJJ just before and after the collapse. At $T < T^*$ the

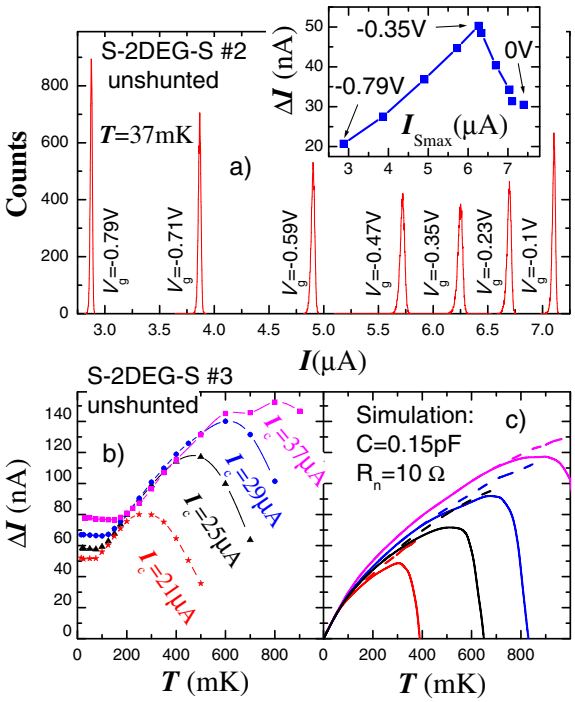

FIG. 2 (color online). Switching statistics of S-2DEG-S: (a) histograms at different V_g for JJ No. 2 at $T = 37$ mK. Inset shows ΔI vs the most probable switching current $I_{S\max}$. A sudden collapse of ΔI occurs at $V_g < -0.35$ V. (b) ΔI vs T for the JJ No. 3 at four magnetic fields, the same as in Fig. 1(b). Three T regions can be distinguished: the MQT at low T, the TA at intermediate T, and collapse of histograms at $T > T^*$. (c) Numerical simulations for the case of Fig. 2(b). Dashed and solid lines represent ΔI for classical TA disregarding and taking into account retrapping, respectively.

histograms are perfectly described by TA [19], shown by the dashed line. However, at $T > T^*$ histograms become narrower and lose the characteristic asymmetric shape.

The observed collapse cannot be explained by T dependence of damping, because Q changes only gradually through T^* and we did take into account $Q(T)$ dependence in the TA prefactor a_t in our simulations. Neither can it be caused by frequency dependent damping due to shunting by circuitry impedance. Indeed, we also observed a similar collapse for planar SNS junctions [23] with $R \simeq 0.2\ \Omega$, for which such shunting plays no role.

We note that T^* is close to T at which hysteresis in IVC's vanishes [cf. Figs. 3(d), 1(d), 2(b), and 1(b)], implying that retrapping plays a role in the collapse. The retrapping rate is known only for underdamped junctions $Q \gg 1$ [2]:

$$\Gamma_R = \frac{I - I_{R0}}{Q_0}\sqrt{\frac{E_{J0}}{2\pi k_B T}}\exp\left[-\frac{E_{J0}Q_0^2(I - I_{R0})^2}{2k_B T}\right]. \quad (2)$$

Here I_{R0} is the fluctuation-free retrapping current. TA retrapping (unlike escape) depends strongly on damping [10] because Q_0^2 appears under the exponent in Eq. (2).

The probability to measure the switching current I is a conditional probability of switching, $P_S(I)$, *and not being retrapped back,* P_{nR}, during the time of experiment.

$$P_{nR} = 1 - \int_I^{I_{c0}} P_R(I)dI, \quad (3)$$

where $P_R(I) = \frac{\Gamma_R(I)}{dI/dt}[1 - \int_I^{I_{c0}} P_R(I)dI]$ is the retrapping probability.

Dash-dotted lines in Figs. 3(a) and 3(b) show the calculated P_{nR}. It is seen that at $T < T^*$ the $P_{nR} = 1$ in the region where $P_S > 0$, therefore retrapping is insignificant. However, at $T > T^*$, retrapping becomes significant at small currents. The resulting conditional probability of measuring the switching current, $P(I) = P_S(I)P_{nR}(I)$, normalized by the total number of switching events, is shown by the solid line in Fig. 3(b). It explains very well both the reduced width and the almost symmetric shape of the measured histogram.

Figures 4(a) and 4(b) represent simulations for the case of S-2DEG-S No. 3, in which we intentionally disregarded T dependencies of I_{c0}, Q_0, and E_{J0}. It is seen that the most probable retrapping current $I_{R\max}$ has a weak T dependence, consistent with the experiment, Fig. 1(b). On the other hand, $I_{S\max}$ decreases approximately linearly with T and eventually crosses $I_{R\max}$. Figure 4(b) shows ΔI, which continuously increases with T for conventional TA, but reduces as soon as the switching and retrapping histograms start to overlap.

The T^* can be estimated from the system of equations:

$$\Gamma_{\rm TA}(I_{S\max}) \simeq (dI/dt)/I_{c0}, \quad (4)$$

$$\Gamma_R(T^*) = \Gamma_{\rm TA}. \quad (5)$$

Equation (4) states that the JJ switches into the R state during the time of experiment. From Eqs. (1) and (4), it follows that $\Delta U(I_{S\max})/k_BT \simeq \ln[\frac{a_t\omega_p I_{c0}}{2\pi dI/dt}] \equiv Y$, which agrees with experiment, as shown in Fig. 4(d). Taking

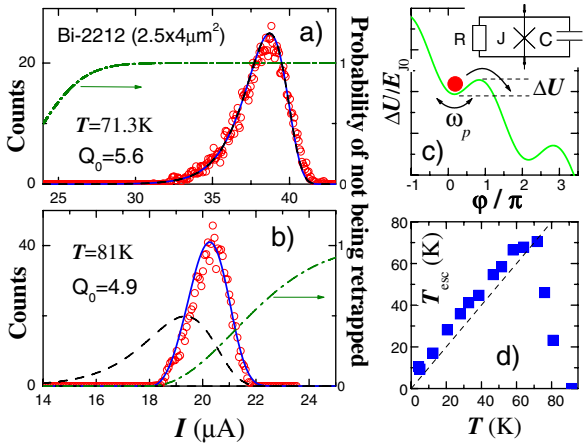

FIG. 3 (color online). Switching histograms of a *single* IJJ at (a) $T < T^*$ and (b) $T > T^*$: dots represent experimental data, dashed lines show TA simulations, and dash-dotted lines show probabilities of not being retrapped. Solid lines show the conditional probability of switching without being retrapped. Note that both the width and the shape of the histograms change at T^*. (c) The tilted washboard potential and the equivalent circuit of the RCSJ model. (d) The effective escape temperature vs T. A sudden collapse of $T_{\rm esc}$ at $T^* \simeq 75$ K is seen.

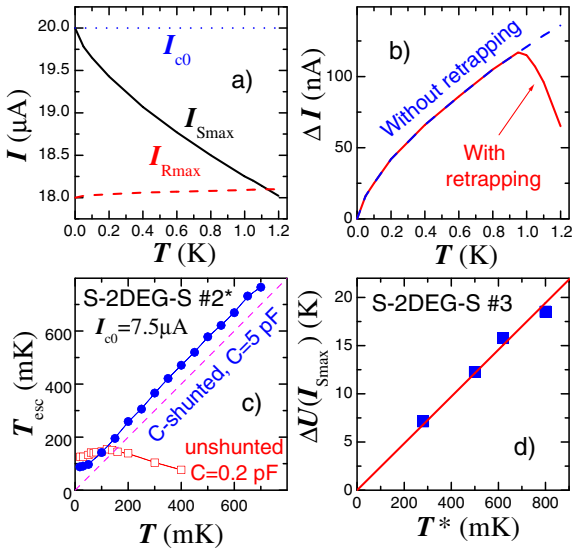

FIG. 4 (color online). (a) Numerical simulations for S-2DEG-S No. 3 for constant $I_{c0} = 20\ \mu$A. T dependencies of the most probable switching $I_{S\max}$ (solid line) and retrapping $I_{R\max}$ (dashed line) currents. (b) The simulated width of histograms disregarding (dashed line) and taking into account (solid line) retrapping. (c) Experimental $T_{\rm esc}$ vs T for S-2DEG-S No. 2* before and after *in situ* C shunting. Dashed line corresponds to $T_{\rm esc} = T$, expected for conventional TA. (d) The height of the escape barrier at $I = I_{S\max}$ vs T^*: symbols represent experimental data from Fig. 2(b), the solid line corresponds to the simulation in Fig. 4(b).

$\Delta U \simeq (4\sqrt{2}/3)E_{J0}[1 - I_S/I_{c0}]^{3/2}$, and neglecting T dependence of I_{c0}, we reproduce the linear T dependence $I_{S\max}/I_{c0} \simeq 1 - (3Yk_BT)/(4\sqrt{2}E_{J0})$, seen in Fig. 4(a). Substituting this expression into Eqs. (2) and (5), and assuming $I_{R0} \simeq \frac{4I_{c0}}{\pi Q_0}$ (valid for $Q_0 > 2$), we get a rough estimation:

$$T^* \simeq \frac{16E_{J0}}{9Q_0^2Y^{1/3}k_B}\left[\sqrt{1 + \left(1 - \frac{4}{\pi Q_0}\right)\frac{3Q_0^2}{\sqrt{8}Y^{1/3}}} - 1\right]^2. \quad (6)$$

From Eq. (6) it follows that T^*/E_{J0} depends almost solely on Q_0. Figure 4(c) shows $T_{\rm esc}$ vs T for a S-2DEG-S No. 2* (similar to No. 2) before and after C shunting. A dramatic difference in the behavior of TA is obvious. As shown in Fig. 1(a) the C shunting affects almost solely Q_0. Therefore, switching to the R state is not strongly affected. On the contrary, retrapping is affected considerably because $I_{R0} \sim 1/Q_0$. Under these circumstances, higher T is required to reduce $I_{S\max}$ to the level of I_R, resulting in the increase of T^*. Similarly, the decrease of Q due to the suppression of I_{c0} causes the collapse of TA vs V_g in Fig. 2(a) and the decrease of T^* with H in Fig. 2(b).

To get an insight into the phase dynamics at $T > T^*$, we show in Fig. 4(d) the dependence of $\Delta U(I = I_{S\max})$ vs T^* for the case of Fig. 2(b). The solid line in Fig. 4(d) corresponds to $\Delta U(I_{S\max})/k_BT = 24.3 \simeq Y$ obtained from simulations presented in Figs. 4(a) and 4(b) and demonstrates excellent agreement with experiment. The large value of $\Delta U/k_BT$ implies that the JJ can escape from the S to the R state only a few times during the time of experiment. Therefore, the collapse is not due to transition into the phase-diffusion state, which may also lead to reduction of ΔI [9]. Indeed, phase diffusion requires repeated escape and retrapping, which is possible only for $\Delta U/k_BT \simeq 1$ [4,24]. Careful measurements of S branches in the IVC's at $T \gtrsim T^*$ did not reveal any dc voltage down to $\sim$10 nV for S-2DEG-S and $\sim 1\ \mu$V for IJJ's. Furthermore, as seen from comparison of Figs. 1(b), 2(b), 1(d), and 3(d), the IVC's remain hysteretic at T well above T^*, which is incompatible with the phase diffusion according to the RCSJ model [4]. As can be seen from Fig. 1(c) the first indication for the phase diffusion in our IJJ's appears only at $T > 90$ K, meaning that all the collapse of TA shown in Fig. 3(c) at $75 < T < 85$ K occurs before entering into the phase-diffusion state.

For a quantitative comparison with experiment we performed full numerical simulations of Eqs. (1)–(3) taking into account the T dependence of I_{c0}, shown in Fig. 1(b) and the exact value of hysteresis I_{c0}/I_{R0} within the RCSJ model. Results of the simulations for the S-2DEG-S No. 3 at four magnetic fields, corresponding to Figs. 1(b) and 2(b), are shown in Fig. 2(c). Dashed and solid lines represent the simulated width of histograms disregarding and taking into account retrapping, respectively. It is seen that simulations quantitatively reproduce T^* for all four magnetic fields. The capacitance $C = 0.15$ pF, which was the only fitting parameter, is the same for all four curves and corresponds to the expected value of stray capacitance. Taking into account that T^* is very sensitive to I_{c0} and C [see Eq. (6)] we may say that the agreement between theory and experiment is excellent.

In conclusion, we observed a paradoxical collapse of thermal activation with increasing T in two very different types of Josephson junctions with moderate damping. The phenomenon was explained by the interplay of two conflicting consequences of thermal fluctuations, which can both assist in premature switching and help in retrapping back into the S state. The retrapping process is significant at small currents, causing cutting off the thermal activation at small bias. We have analyzed the influence of dissipation on the thermal activation by tuning the damping parameter with the gate voltage, magnetic field, temperature, and *in situ* capacitive shunting. Numerical simulations are in good agreement with experimental data and explain both the paradoxical collapse and the unusual shape of switching histograms.

[1] P. Hänngi *et al.*, Rev. Mod. Phys. **62**, 251 (1990).
[2] E. Ben-Jacob *et al.*, Phys. Rev. A **26**, 2805 (1982).
[3] H. Grabert *et al.*, Phys. Rev. B **36**, 1931 (1987).
[4] R. L. Kautz and J. M. Martinis, Phys. Rev. B **42**, 9903 (1990).
[5] S. Washburn *et al.*, Phys. Rev. Lett. **54**, 2712 (1985).
[6] J. M. Martinis *et al.*, Phys. Rev. B **35**, 4682 (1987).
[7] P. Silvestrini *et al.*, Phys. Rev. Lett. **60**, 844 (1988).
[8] E. Turlot *et al.*, Phys. Rev. Lett. **62**, 1788 (1989).
[9] D. Vion *et al.*, Phys. Rev. Lett. **77**, 3435 (1996).
[10] M. G. Castellano *et al.*, J. Appl. Phys. **80**, 2922 (1996).
[11] M. Schlosshauer, Rev. Mod. Phys. **76**, 1267 (2005).
[12] R. McDermott *et al.*, Science **307**, 1299 (2005); A. J. Berkley *et al.*, *ibid.* **300**, 1548 (2003).
[13] I. Chiorescu *et al.*, Nature (London) **431**, 159 (2004).
[14] D. Vion *et al.*, Science **296**, 886 (2002).
[15] At the final stage of preparation of this manuscript we noticed another work, J. M. Kivioja *et al.*, Phys. Rev. Lett. **94**, 247002 (2005), with similar observations and an explanation similar in spirit but different in details.
[16] H. Takayanagi *et al.*, Phys. Rev. Lett. **75**, 3533 (1995); T. Akazaki *et al.*, Appl. Phys. Lett. **86**, 132505 (2005).
[17] T. Bauch *et al.*, Phys. Rev. B **71**, 174502 (2005).
[18] V. M. Krasnov *et al.*, Phys. Rev. Lett. **84**, 5860 (2000); **86**, 2657 (2001); Phys. Rev. B **65**, 140504(R) (2002).
[19] V. M. Krasnov *et al.*, Phys. Rev. B **72**, 012512 (2005).
[20] RCSJ model describes IJJ's only at elevated T.
[21] T. A. Fulton and L. N. Dunkleberger, J. Appl. Phys. **45**, 2283 (1974).
[22] Y. Song, J. Appl. Phys. **47**, 2651 (1976).
[23] V. M. Krasnov *et al.*, Physica (Amsterdam) **418C**, 16 (2005).
[24] A. Franz *et al.*, Phys. Rev. B **69**, 014506 (2004); P. A. Warburton *et al.*, J. Appl. Phys. **95**, 4941 (2004).